

## Determination of Local Tissue Enhancement from Radially Reconstructed Images

Jennifer Moroz<sup>1</sup>, Piotr Kozłowski<sup>2,3</sup>, and Stefan A Reinsberg<sup>1</sup>

<sup>1</sup>Physics and Astronomy, UBC, Vancouver, BC, Canada, <sup>2</sup>Radiology, UBC, Vancouver, BC, Canada, <sup>3</sup>MRI Research Centre, UBC, Vancouver, BC, Canada

**Target audience:** This project will benefit any individual in the field of Dynamic Contrast-Enhanced (DCE) MRI, particularly those who model the DCE data with an arterial input function (AIF).

**Purpose:** The arterial input function (AIF) is a required input parameter for pharmacokinetic modelling [1]. For accurate modelling, the AIF should be sampled at sufficiently high spatial and temporal resolutions to avoid partial volume effects (PVE) [2] and to capture the rapid contrast kinetics in blood [3]. Our group recently proposed a projection-based AIF measurement (in a mouse tail) in which the AIF is determined from the change in signal phase from a series of projections [4]. However, the accuracy of this technique may be limited by contrast perfusion from the vascular space into the surrounding tissue. Such perfusion will result in local enhancement of the tissue, thus leading to additional changes to the profile of the projection not related to a change in the vascular concentration of contrast agent. Tissue enhancement may be measured through the construction of a series of MR images. To maintain the high temporal-resolution of our AIF, radial images are desired. The goal of this work is to evaluate our ability to measure local tissue enhancement. Through simulations, the method of radial reconstruction best suited for measuring local tissue enhancement may be determined, as well as the minimum number of radial spokes required for accuracy.

**Methods:** Data acquisition took place on a Biospec 70/30 Bruker 7.0 T MRI system. A phantom mimicking a mouse tail - a capillary tube (inner diameter 0.4 mm, filled with 2 mM Gd mixed in 0.9% saline) placed within a glass tube (internal diameter 3.7 mm, filled with tap water) - was centered in the magnet. A birdcage coil (inner diameter 7.0 cm) was used for signal excitation and an actively decoupled surface coil (width 7 mm, length 18 mm) was used for data collection. A FLASH experiment was performed (TR/TE = 100 ms/3.927 ms, flip angle = 30°, 1.5x1.5 cm<sup>2</sup> FOV, matrix size 256x256) to construct a 2-D Cartesian Image. Radial projections were obtained through application of the forward Radon transform function in MATLAB (Mathworks, Inc.) for angles 1-360° in 1° increments.

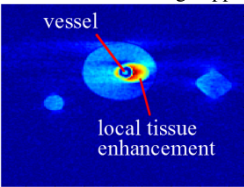


Figure 1: Image of phantom with local tissue enhancement.

Images of these radial projections were reconstructed using three methods: 1) Regriding the data onto a Cartesian grid using Shepard's method of interpolation [5], (with no filtering of the k-space data prior to applying the FFT, and with filtering of k-space with a Kaiser-Bessel filter) 2) Spatial-Temporal Constrained Reconstruction (STCR) [6,7], and 3) the Non-equidistant Fast Fourier Transform (NFFT) [8]. Images were constructed with varying numbers of equally spaced radial projections ranging from 180 (full data set) to 18. Image quality was assessed with the signal-to-noise (SNR) ratio and the contrast-to-noise (CNR) ratio of the phantom. To evaluate the potential for each method to accurately model tissue enhancement, a 'leak' was initiated at the boundary of the phantoms' vessel (Figure 1). The leak profile is Gaussian in shape and expanded outward as an ellipsoid. The maximum intensity of the enhancement is described by:

$$\text{Enhancement Magnitude} = \begin{cases} e^{-(p-400)^2/25000} & p < 400 \\ 1.75 - 1.5 / \left(1 + e^{-\frac{(p-400)^2}{100000}}\right) & p \geq 400 \end{cases}$$

where  $p$  is the projection number in the series. This equation was chosen to approximate the enhancement of tissue background roughly following the shape of an AIF, but occurring on a slower time scale relative to the changes experienced in the vasculature. A total of 1080 projections were used in the subsequent analysis. Images were reconstructed with a sliding window of 36 radial projections for the three methods described above (spaced 111° apart [9] for Shepard's interpolation and STCR, and 115° for NFFT as this angular spacing produced streak-free images). The leak profile was isolated from the image through subtraction of the baseline image, and then summed along the phase-encode direction. An error profile ((reconstructed-expected)/expected) was calculated to assess errors in the profile resulting from the different reconstruction methods. The mean  $\pm$  standard deviation of all error profiles was calculated in the region of enhancement and in the region of the vessel.

**Results:** Images reconstructed with the regriding technique (no filter) were visually comparable with the reference Cartesian image when 180 or more radial projections were used. Despite the fact that the SNR and CNR for these images were comparable for images with 36 or more projections, object details (edges and intensity gradients) became blurred as the number of projections was reduced. Filtering k-space with the Kaiser-Bessel filter improved the quality of the reconstruction, such that images created with as few as 36 radial projections resembled the Cartesian image. Images of the enhancement profile (not shown) revealed that the difference was greatest at the centre of the enhancement, where the intensity was highest (23.7% difference (no filtering) or 20.8% difference (Kaiser-Bessel filter used)). The error profile (Figure 2, a and b) had the largest values when the enhancement region was small and of very low intensity. Mean errors in the enhancement and vessel regions were (21.3  $\pm$  6.3)% and (12.7  $\pm$  2.3)% with no filter and (32.8  $\pm$  7.9)% and (16.2  $\pm$  5.7)% for the filtered images. The STCR technique reproduced the phantom with high accuracy for the static case, but produced ghosting artifacts along the edges of the leak when the magnitude of enhancement was high. Images of the enhancement profile also showed the greatest differences at the centre of the enhancement region. The maximum error in the error profile (Figure 2, c) appeared to depend on the maximum intensity of enhancement, reaching a maximum around projection 400. The mean errors in the enhancement and vessel regions were (12.2  $\pm$  5.2)% and (7.8  $\pm$  1.1)%. The magnitude images of the NFFT reconstruction differed from the reference Cartesian image as the reference phantom had relatively lower intensity compared to the capillary. Despite this, the NFFT technique produced the best estimate of the enhancement profile (Figure 2, d), with mean errors of (10.9  $\pm$  2.9)% and (5.8  $\pm$  1.8)% in the enhancement and vessel regions, respectively.

**Discussion:** Local tissue enhancement will limit the utility of a projection-based AIF in a mouse tail and should be accounted for. This simulation-based study attempted to identify which method of radial image reconstruction will

best approximate changes in the projection profile resulting from local tissue enhancement. The results of this analysis suggest that the NFFT technique may be best suited for our application, providing the lowest error in the region of the vessel, especially when the enhancement region was small and had low intensity. For this analysis, images were constructed with only 36 projections (3.6 s temporal resolution) as this number produced images similar to the Cartesian standard. However, depending on the repetition time used and rate of tissue enhancement, a larger number of projections could be used to improve the results.

**Conclusion:** The results suggest that the NFFT method for radial reconstruction is superior to STCR and regriding, using Shepard's method of interpolation, for estimating local tissue enhancement. Mean errors in the projection profile were less than 6% in the region of the vessel, whereas the other two methods showed errors in excess of 100% when the enhancement magnitude was low (i.e. at the start of enhancement).

**Acknowledgements:** This work was made possible by support from NSERC and the Canadian Cancer Society.

**References:** [1] Knutsson et al, *Mag Reson Mater Phys*, 23: 1-21, 2010, [2] Hansen et al. *MRM*, 62: 1055-1059, 2009, [3] Garpebring et al, *MRM*, 65: 1670-1679, 2011, [4] Moroz et al., *Proc. Intl. Soc. Mag. Reson., Med.*, 20: 239, 2012, [5] Shepard, *Proc. 1968 ACM Nat. Conf.*, p. 517-524, 1968, [6] Adluru, et al. *JMRI*, 29: 466-473, 2009, [7] <http://www.sci.utah.edu/bisti.html>, [8] Keiner et al. *ACM Trans Math Software*, 36: 1-30, 2009, [9] Winkelmann et al. *IEEE Trans Med Imag*, 26: 68-76, 2007.

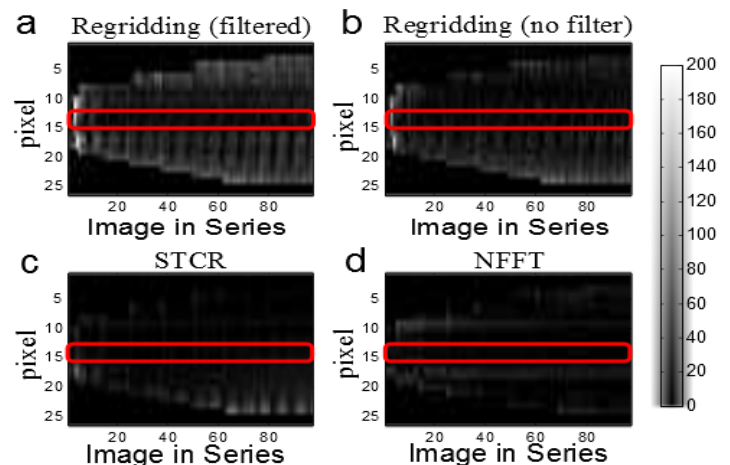


Figure 2: Error profiles, showing percent difference from expected profile, of the tissue enhancement region for regriding with Shepard's method of interpolation, (a) with and (b) without filtering k-space, (c) STCR and (d) the NFFT. The vessel region is outlined in red.